Retrograde signalling in depolarization-induced suppression of inhibition in rat hippocampal CA1 cells

B. E. Alger, T. A. Pitler, J. J. Wagner, L. A. Martin, W. Morishita, S. A. Kirov and R. A. Lenz

Department of Physiology, University of Maryland School of Medicine, Baltimore, MD 21201, USA

1. We have investigated the phenomenon of 'depolarization-induced suppression of inhibition' (DSI) using whole-cell voltage-clamp techniques in CA1 pyramidal cells of rat hippocampal slices. DSI was induced by eliciting voltage-dependent calcium (Ca^{2+}) currents with 1 s voltage steps of +60 to +90 mV from the holding potential. DSI was apparent as a reduction in synaptic $GABA_A$ responses for a period of about 1 min following the voltage step.

2. TTX-sensitive spontaneous IPSCs (sIPSCs) were susceptible to DSI, while TTX-resistant miniature inhibitory postsynaptic currents (mIPSCs) were not. Miniature IPSCs are ordinarily infrequent and independent of external Ca^{2+} in the CA1 region. To increase the frequency of mIPSCs and to induce a population of Ca^{2+}-sensitive mIPSCs, we increased the bath K^+ concentration to 15 mM. The increased mIPSCs were also insensitive to DSI, however.

3. The whole-cell pipette-filling solution contained 5 mM 2(triethylamino-*N*-(2,6-dimethylphenyl)acetamide (QX-314) to block voltage-dependent Na^+ currents and caesium to block K^+ currents. Nevertheless, bath application of 50 μM 4-aminopyridine (4-AP) or 250 nM veratridine both clearly reduced DSI, evidently by acting at presynaptic sites.

4. The amplitudes of monosynaptically evoked IPSCs (elicited in the presence of 10 μM 6-cyano-7-nitroquinoxaline-2,3-dione (CNQX) and 50 μM 2-amino-5-phosphonovaleric acid (APV)) were dramatically reduced during the DSI period. Weak stimulation produced small IPSCs and occasional 'failures' of transmission during the control period. The percentage of failures increased markedly during the DSI period. Moderate-intensity stimulation produced larger IPSCs that were often composed of distinguishable multiquantal components. All-or-none failures of multiquantal IPSC components also occurred during DSI.

5. The degree of paired-pulse IPSC depression did not change during DSI, whereas it was decreased, as expected, by baclofen.

6. We conclude that the data represent novel evidence that DSI is mediated by a retrograde signalling process possibly involving presynaptic axonal conduction block.

Transient depolarizations, via brief trains of action potentials or voltage steps, of hippocampal pyramidal cells (Pitler & Alger, 1992*a*; Pitler & Alger, 1994*b*) and cerebellar Purkinje cells (Vincent, Armstrong & Marty, 1992; Vincent & Marty, 1993) suppress $GABA_A$ergic inhibitory postsynaptic currents (IPSCs) for 30–120 s. This phenomenon, depolarization-induced suppression of inhibition (DSI), is important because decreases in efficacy of $GABA_A$ergic inhibition promote the induction of long-term potentiation (Wigstrom & Gustafsson, 1983; Stelzer, Simon, Kovacs & Rai, 1994) as well as the onset of certain types of epileptic activity (Stelzer, 1992; McNamara, 1994).

It has been suggested that DSI involves depression of GABA release mediated by a retrograde signal (see Alger & Pitler, 1995, for review). DSI is clearly induced by postsynaptic factors. It can be initiated by activity that is restricted to the postsynaptic cell and blocked by strongly buffering rises in intracellular calcium ($[Ca^{2+}]_i$) with the calcium chelator, BAPTA (Llano, Leresche & Marty, 1991; Pitler & Alger, 1992*a*). While decreases in postsynaptic $GABA_A$ receptor sensitivity could in principle explain DSI (Chen, Stelzer, Kay & Wong, 1990) decreased $GABA_A$ receptor sensitivity has not been detected either by iontophoretic GABA application (Llano *et al.* 1991; Pitler & Alger, 1992*a*) or by

an analysis of spontaneous TTX-resistant miniature IPSCs (mIPSCs; Llano *et al.* 1991; Pitler & Alger, 1994*b*). If DSI is induced by postsynaptic factors and yet not explained by them, the locus of DSI expression must be presynaptic. Indeed, in cerebellum an increase in 'failures' of evoked quantal release during DSI (Vincent *et al.* 1992) and evidence for a TTX-sensitive propagation of DSI from one Purkinje cell to another (Vincent & Marty, 1993) also support a presynaptic locus. If DSI is expressed at a presynaptic site then a retrograde signalling process would be implied.

However, some issues remain unresolved. Even if mIPSCs are true quanta (Edwards, Konnerth & Sakmann, 1990; Edwards, 1991), the strength of the spontaneous mIPSC data depends on whether or not the mIPSCs originate at the same synapses as those at which DSI occurs. DSI could conceivably be caused by decreased $GABA_A$ receptor sensitivity only at the susceptible synapses. Because spontaneous mIPSC frequency is often low (~1 Hz) in hippocampus, and the number of $GABA_A$ synapses is very high, many synapses may not experience significant spontaneous quantal release (cf. Soltesz, Smetters & Mody, 1995). If DSI occurred only at silent synapses, conclusions based on spontaneous mIPSCs would be invalid.

Furthermore, apparent failures of quantal transmitter release arising from presynaptic causes would be difficult to distinguish from a hypothetical mechanism involving regulation of transmission at the level of a small receptor cluster, such as those that probably characterize $GABA_A$ synapses in the CNS (Edwards *et al.* 1990; Edwards, 1991). The ten to thirty receptors in a patch that are activated by a quantum of transmitter could be switched between responsive and non-responsive states, perhaps by a phosphorylation–dephosphorylation process (Chen, Stelzer, Kay & Wong, 1990). Switching a cluster off would be indistinguishable from a presynaptic failure of transmitter release.

Although cerebellar DSI shares several common characteristics with hippocampal DSI (Alger & Pitler, 1995), they do differ in some respects. In hippocampus, spontaneous IPSCs (sIPSCs) are Ca^{2+} dependent while mIPSCs are not (Thompson, 1994) and TTX-resistant mIPSCs in hippocampus are small and resistant to DSI. In cerebellum TTX-resistant IPSCs are large, Ca^{2+} dependent and susceptible to DSI. Considering these fundamental differences, it is not entirely clear to what extent generalizations concerning DSI mechanisms from each structure are valid.

Finally, our previous conclusions in favour of a presynaptic expression site for DSI were based on negative evidence: since there was no indication of a postsynaptic reduction in $GABA_A$ receptor responsiveness, DSI would have to be explained by presynaptic factors. More direct tests of the retrograde signalling hypothesis are necessary.

We have undertaken the present experiments to address these issues. The new evidence strongly supports the hypothesis that DSI is mediated via a retrograde signalling process. A preliminary report of this work has appeared (Pitler, Alger, Wagner & Lenz, 1995).

METHODS

Preparation of slices

Adult male Sprague–Dawley rats (125–250 g) were anaesthetized with halothane and decapitated, the brain was removed and both hippocampi were dissected free. After being placed on an agar block in a slicing chamber containing partially frozen saline, the hippocampus was sectioned transversely at 400 μm intervals with a Vibratome (Oxford). The slices recovered in a holding chamber at the interface of a physiological saline and humidified 95% O_2–5% CO_2 atmosphere at room temperature. After a minimum 1 h incubation, a single slice was transferred to a submerged, perfusion-type chamber (Nicoll & Alger, 1981) where it was perfused at ~0·5 ml min^{-1} at 29–31 °C.

Solutions

Patch electrodes with resistances of 3–6 MΩ were filled with (mM): 145–160 CsCl, 2 BAPTA, 0·2 $CaCl_2$, 1 MgATP, 1 $MgCl_2$, 5 2(triethylamino)-*N*-(2,6-dimethylphenyl)acetamide (QX-314), 10 Hepes and 0·3 Tris-GTP (pH = 7·35). In a few cells, as noted, KCl or KCH_3SO_3 replaced CsCl. Extracellular saline contained (mM): 124 NaCl, 25 $NaHCO_3$, 3·5 KCl, 2 $CaCl_2$, 2 $MgCl_2$, 1·25 NaH_2PO_4 and 10 glucose. 6-Cyano-7-nitroquinoxaline-2,3-dione (CNQX; 10 μM) and 2-amino-5-phosphonovaleric acid (APV; 50 μM) were present in all experiments to block ionotropic glutamate responses. Carbachol (25 μM) enhances sIPSCs (Pitler & Alger, 1992*b*) and DSI of sIPSCs (Pitler & Alger, 1992*b*) and was present for all experiments on sIPSCs or mIPSCs, but not for experiments on evoked IPSCs.

CNQX was purchased from Research Biochemicals International, BAPTA from Molecular Probes and TTX from Calbiochem. QX-314 was a generous gift from Astra (Södertalje, Sweden) or was purchased from Alamone Labs (Jerusalem). All other drugs and chemicals were obtained from Sigma. All drugs were bath applied.

Whole-cell recordings and data analysis

CA1 pyramidal cell recordings were obtained using the 'blind', whole-cell patch-clamp recording technique (Blanton, Lo Turco & Kriegstein, 1989). Cells were voltage clamped near their resting potential immediately after break-in. Acceptable cells had resting potentials >-55 mV and input resistances >40 MΩ. Series resistance was <12 MΩ at the beginning of an experiment and compensated by ~80%. Cells were discarded if series resistance increased to >20 MΩ during an experiment. Liquid junction potentials were small and were not corrected for. Evoked IPSCs were filtered at 2 or 3 kHz and stored on VHS videotape. Responses were digitized at 10 or 20 kHz and analysed with pCLAMP 6.0 (Axon Instruments).

DSI of sIPSCs and KCl-induced mIPSCs was quantified in some experiments by integrating (using the Fetchan subroutine of pCLAMP) the current traces over 1 or 2 s time bins for periods of at least 8 s directly preceding and following the depolarizing current pulse delivered to induce DSI. This gives a measure of total charge crossing the membrane and is a robust index of the amount of synaptic activity present. Spontaneous IPSC data were filtered at

1 kHz and digitized at 2 kHz. The baseline for integration of each trace was set manually, and rigorous visual inspection of all traces was performed to ensure that the analysis was not corrupted by the presence of events with aberrant waveforms, by periods of unstable holding current fluctuation or by noise. The quantitative results using this method faithfully agreed with the conclusions based on visual inspection of the data.

In other cases, the amplitude and latency of individual events were measured from cursor measurements in the Clampfit subroutine of pCLAMP. Evoked IPSCs were elicited at 0·5 or 1 Hz continuously. Traces were captured in Clampex (version 6.03, Axon Instruments), smoothed with a five-point running mean to reduce the noise variance and the peak amplitudes measured with respect to baseline immediately before the onset of the stimulus artifact in Clampfit. Latencies were determined from cursor measurements as the time between the onset of the stimulus artifact and the earliest onset of the IPSC. In the case of complex IPSCs having multiple components (see text) the latency was measured to the earliest onset of the component determined either from the differentiated waveform as the point at which the derivative clearly began to change or as the inflection point in the undifferentiated trace. It was repeatedly confirmed that these two methods of determining latency agreed. The square of the coefficient of variation (CV^2) of evoked IPSCs was determined as the variance of the peak amplitude fluctuations compared with the square of the mean peak IPSC amplitude for each cell. As detailed in the text, evoked IPSCs were large (mean, -572 ± 120 pA). Correction for baseline variance, recommended for CV^2 analysis of quantal events (Faber & Korn, 1991), was negligible for these large IPSCs ($3{\cdot}3 \pm 1{\cdot}5\%$ in three cells) and hence was not performed for the data shown. To analyse changes during DSI, we measured IPSCs that occurred during the interval of maximal suppression, usually twelve events beginning at the third pulse following the DSI step. As previously shown (Pitler & Alger, 1994*b*), maximal DSI typically takes 1–3 s to develop after the step. We compared the mean amplitude of IPSCs evoked during this DSI interval with that of the same number of IPSCs during the control period immediately preceding the DSI-inducing voltage step. Statistical significance was assessed by two-tailed t tests with a significance level of $P \leqslant 0{\cdot}05$.

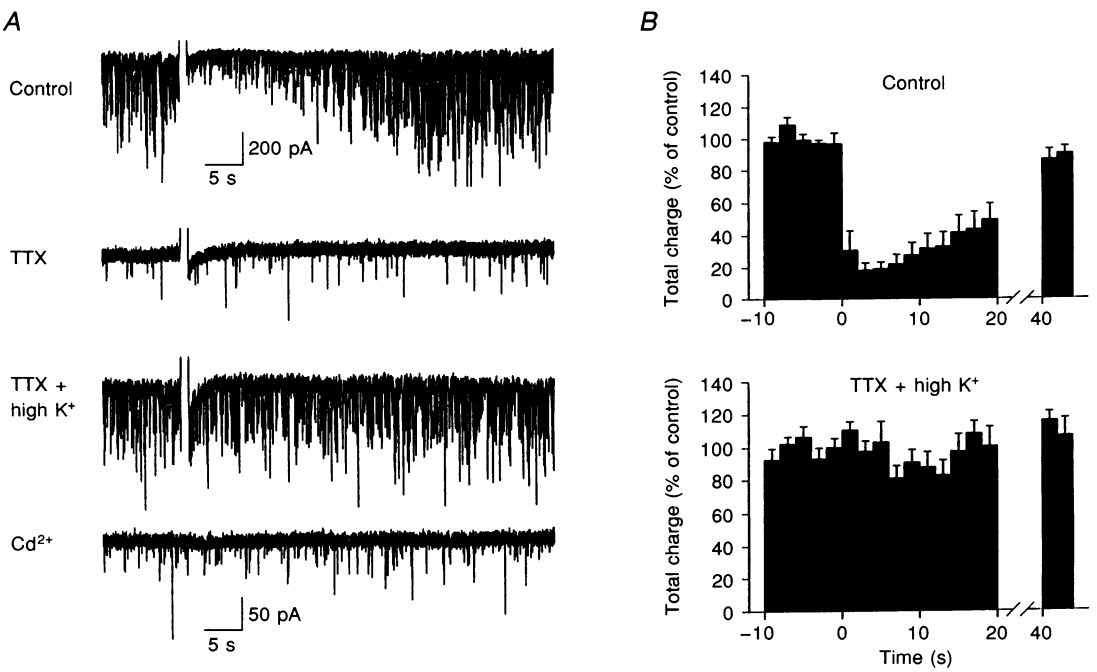

Figure 1. Depolarization-induced suppression of inhibition (DSI) does not affect TTX-resistant miniature inhibitory postsynaptic currents (mIPSCs)

A, whole-cell voltage-clamp recording of a CA1 pyramidal cell recorded with a KCl-containing pipette and bathed in solution containing 10 μM CNQX, 50 μM APV and 25 μM carbachol (see Methods). The downward deflections are $GABA_A$-mediated spontaneous IPSCs. At the interruption in the traces the membrane potential was stepped from −60 to +10 mV for 1 s (top trace). The period of sIPSC depression represents DSI. Addition of tetrodotoxin (TTX; 0·3 μM) to the bath blocked the large sIPSCs and revealed TTX-resistant mIPSCs that are not susceptible to DSI (second trace from top). Adding 15 mM KCl to the bath greatly increased the numbers of mIPSCs, but all remained resistant to DSI (third trace from top). Further addition of 250 μM $CdCl_2$ blocked most of the mIPSCs induced by high K^+, indicating that they were Ca^{2+} dependent (bottom trace). All traces are from the same cell. Bottom calibration bar applies to lowest three traces. *B*, the results in *A* are typical of data from 3 cells recorded with CsCl-based electrode filling solution and 4 cells with a KCl-based solution. The amount of spontaneous activity was quantified by integrating the current traces in 2 s bins (see Methods). The results are expressed as total charge crossing the membrane, normalized to the mean of the 10 s control period prior to the DSI pulse which was given at time zero. Group data from all 7 cells are plotted in the histograms.

RESULTS

TTX-insensitive miniature IPSCs are not blocked by DSI

We investigated DSI expression with whole-cell voltage-clamp techniques in CA1 pyramidal cells of the rat hippocampal slice. Figure 1 illustrates data from a cell in which DSI of sIPSCs, induced by a 1 s, 70 mV voltage step to +10 mV, was apparent in control conditions prior to adding TTX to the bath. TTX rapidly abolished the large sIPSCs, leaving mIPSCs, which are not affected during the DSI period in hippocampus (Pitler & Alger, 1994*b*). The effects of TTX were evidently exerted presynaptically, since postsynaptic Na^+ currents had been blocked by the QX-314 in the recording electrode (see Methods). Adding 15 mM KCl to the TTX-containing bathing solution increased mIPSC frequency approximately 10-fold and induced the appearance of Ca^{2+}-dependent mIPSCs by activating voltage-dependent Ca^{2+} channels in individual GABAergic nerve terminals (Doze, Cohen & Madison, 1995). The DSI protocol remained ineffective in suppressing the mIPSCs. The final trace in Fig. 1 illustrates that many of the K^+-induced mIPSCs are sensitive to Cd^{2+}, thus confirming that they were Ca^{2+} dependent. Hence, neither increased numbers nor the presence of Ca^{2+}-dependent mIPSCs reveal evidence of a postsynaptic component of DSI expression.

Bath application of 4-AP or veratridine reduces DSI

As a direct test of presynaptic expression, we attempted to influence DSI, in saline with normal $[K^+]$, with agents that affect synaptic transmission presynaptically. At 50–100 μM, 4-AP preferentially blocks a transient, voltage-dependent K^+ current called 'I_D' in the hippocampus (Storm, 1988) and thereby increases synaptic transmission. DSI was reversibly reduced by 50 μM 4-AP ($n = 6$; Fig. 2). The DSI process reduced IPSC activity by 72 ± 3% in the control conditions, by 18 ± 6% during 4-AP perfusion and by 58 ± 9% following washout of 4-AP. The reduction of DSI by 4-AP was significant ($P < 0{\cdot}001$) and was seen with KCl ($n = 3$) or CsCl ($n = 3$) in the recording pipettes. As expected, 4-AP had no effect on holding current or cell input conductances, because the CsCl and QX-314 in our recording pipettes block postsynaptic K^+ channels. Thus the inhibition of DSI by 4-AP was exerted presynaptically.

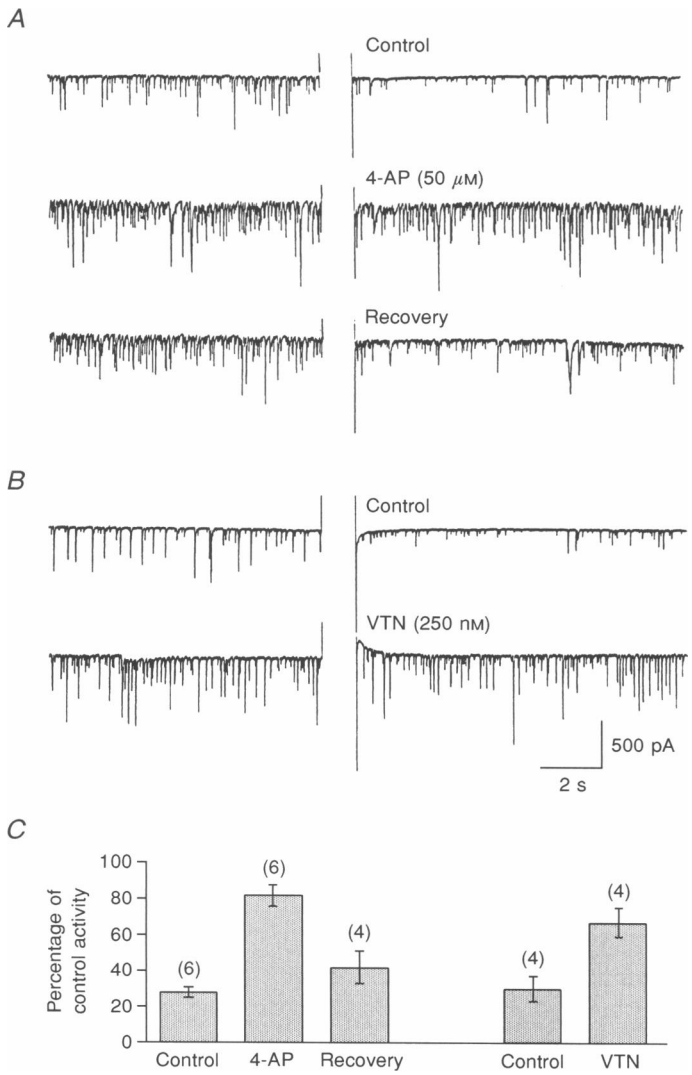

Figure 2. DSI can be reduced by pharmacological agents that act presynaptically

Each trace depicts 10 s of sIPSCs prior to delivery of a 1 s voltage step from −60 to +20 mV, and then 10 s of activity immediately following the pulse. DSI is the reduction in activity following the pulse. Recovery from DSI occurred after the end of the portion of the traces illustrated (not shown). *A*, DSI was induced several times in control solution (e.g. top trace). Bath application of 50 μM 4-AP for 10 min reversibly reduced DSI (middle trace and bottom). *B*, DSI in another cell was tested in control (top) and then again 10 min after adding 250 nM veratridine (VTN) to the bathing solution (bottom trace). Veratridine blocked DSI; its effects were not reversed despite up to 30 min of washing (not shown). *C*, for each experiment done as in *A* (three bars on left) or *B* (two bars on right), the activity in 4 complete DSI trials (control and DSI period) was calculated and averaged. DSI was quantified as in Fig. 1. Histogram represents means ± S.E.M. from the number of cells shown in parentheses.

We also used the Na^+ channel agonist veratridine, which, by prolonging the open time of voltage-dependent Na^+ channels, can enhance neurotransmitter release (Cutler & Young, 1979). Veratridine, bath-applied at 250 nM, reduced DSI ($n = 4$; Fig. 2). The DSI process reduced IPSC activity by $70 \pm 7\%$ in the control saline, but only by $33 \pm 8\%$ during veratridine perfusion. The difference in the degree of IPSC suppression is statistically significant ($P < 0{\cdot}02$). The effects of veratridine could not be reversed with up to 30 min of washing. Like 4-AP, veratridine must have acted presynaptically, since postsynaptic voltage-dependent Na^+ channels were blocked by QX-314 in the recording pipette.

Monosynaptically evoked IPSCs are also blocked during DSI

While the pharmacological tests point to a presynaptic site of DSI expression, more direct evidence was desirable. We therefore studied DSI of monosynaptically evoked IPSCs (Davies, Davies & Collingridge, 1990) in the presence of 10 μM CNQX and 50 μM APV. Monosynaptically evoked IPSCs were elicited continuously at 0·5 Hz with an extracellular stimulating electrode in the vicinity of the recording pipette. Initially, the repetitive stimulation resulted in a modest decline in the monosynaptic IPSC amplitude of 20–30% (not shown) perhaps caused by the activation of $GABA_B$ autoreceptors on the GABA-releasing neuron terminal (Davies *et al.* 1990), but after several seconds the evoked IPSC stabilized. Thereafter, at intervals of 90 or 120 s (in different cells), we interposed a 1 s DSI-inducing voltage step into the on-going series of evoked monosynaptic IPSCs. Following the step the evoked IPSCs were depressed with a time course similar to DSI of sIPSCs (e.g. Fig. 3). In general, DSI of evoked IPSCs is less readily observed (approximately 30–40% of cases) than DSI of spontaneous IPSCs in the presence of carbachol, which occurs in over 80% of stable cells (e.g. Pitler & Alger, 1994*b*). The reasons for this difference are not clear and will be addressed in future experiments.

Analysis of the coefficient of variation (CV) of synaptic responses is often used to help distinguish between presynaptic and postsynaptic sites of changes in synaptic transmission. Generally, if CV^2 does not change following an experimental treatment that altered synaptic responses, then a postsynaptic site is indicated, whereas a change in CV^2 may indicate a presynaptic site (see Discussion). We analysed CV^2 of evoked IPSCs from eleven cells prior to and during the DSI period (see Methods). While the response range was large (−233 to −1569 pA with a mean ± S.E.M. of -572 ± 120 pA), the CV values were fairly constant, $-0{\cdot}20 \pm 0{\cdot}02$. DSI caused a mean $35{\cdot}3 \pm 4{\cdot}3\%$ suppression of the IPSCs (range, 17·3–56·5%) in this group. On average, the CV increased during DSI to $-0{\cdot}27 \pm 0{\cdot}03$, although in two cells CV actually decreased during DSI (DSI in these two cells was 51 and 22%). In Fig. 4, the ratio of CV^2 in control (CV_c^2) to CV^2 during DSI (CV_d^2) is plotted on the y-axis *versus* the ratio of the means of IPSC amplitudes during DSI ($IPSC_d$) to those in control ($IPSC_c$) on the x-axis. Points following on or below the diagonal ('region II_d' of Faber & Korn, 1991) are consistent with a purely

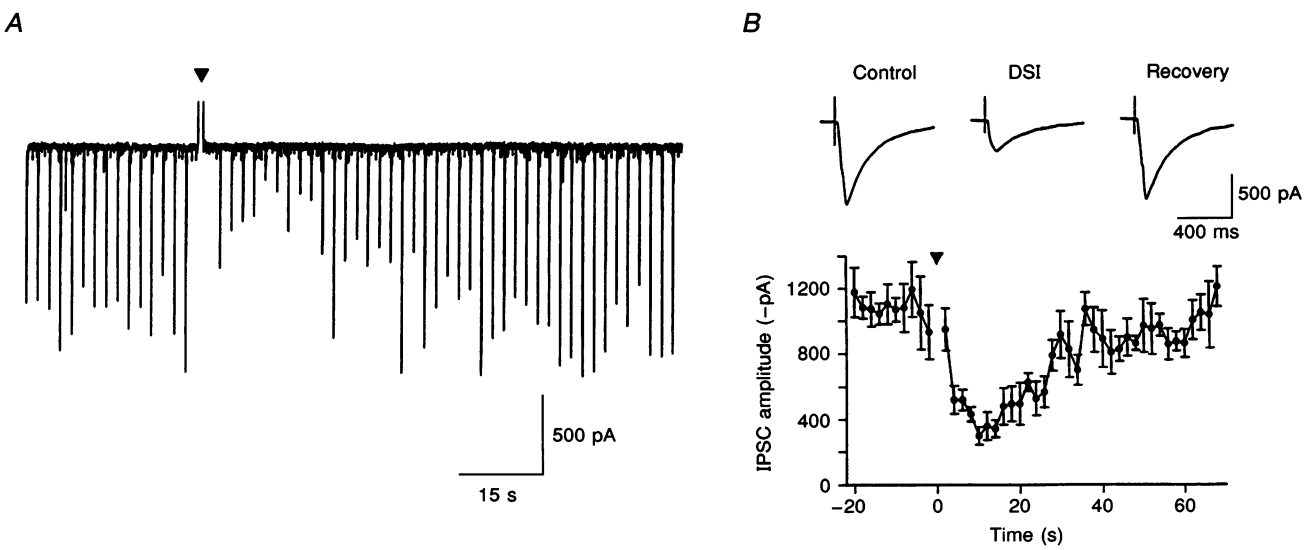

Figure 3. Evoked monosynaptic IPSCs are susceptible to DSI

IPSCs were recorded under whole-cell voltage clamp in the presence of 10 μM CNQX and 50 μM APV (carbachol was not present) with CsCl-containing pipettes. IPSCs were elicited continuously at 0·5 Hz with extracellular electrical stimulation in the vicinity of the recorded cell. At 90 s intervals a 1 s 70 mV depolarizing voltage step from −60 mV was delivered (arrowhead at time zero) to the pyramidal cell. *A*, a typical complete DSI trial on an evoked IPSC (downward strokes, note time scale). *B*, combined data from same cell as in *A*. Traces at the top are averages of 5 responses each in control conditions (prior to the DSI pulse), during the DSI period and following recovery from DSI. The graph shows the entire time course from this experiment; each point represents the mean ± S.E.M. of 5 responses.

presynaptic mechanism. The points on the graph near the diagonal or in region II_d represent the nine cells in which CV increased during DSI (filled circles). The two points above the horizontal line represent those points in which CV decreased during DSI. (One of those above the line is from the experiment depicted in Fig. 7*A*. In this case, it is clear that the dropout of the large second component during DSI results in a greater decrease in the variance than in the mean response, and hence CV_c^2/CV_d^2 increases.) The mean of all eleven points (open triangle) falls on the diagonal. The data are consistent with the assignment of a presynaptic locus for DSI expression.

DSI involves 'failures' of minimally evoked synaptic transmission

Despite the indication from the CV^2 analysis, our system is complex, and interpretation of the results could be complicated. Tests of the 'reliability' of transmission, i.e. whether a given stimulus elicits transmitter release or not, are recommended for analysis of transmission because release is controlled in the presynaptic nerve terminal (Faber & Korn, 1991).

We attempted to elicit quantal-sized IPSCs (20–50 pA) with weak stimulation to assess possible changes in reliability of transmission during DSI, but often found it difficult to evoke IPSCs of this size consistently; even with weak stimulation, responses could vary by up to several hundred picoamps. With careful placement of the stimulating electrode in str. radiatum and adjustment of stimulation intensity we were able to obtain recordings of very small evoked, evidently quantal, IPSCs that failed frequently with 0·5 Hz stimulation in the control period. An example of one such experiment is shown in Fig. 5*A* and in group data for the failure rate before and during DSI in Fig. 5*B*. During the DSI period, the failure rate in three cells rose from 12 ± 6·1 to 86 ± 3·4%. These results thus supported the hypothesis of a presynaptic locus of DSI expression.

DSI involves failures of multiquantal IPSCs

In the case of the glutamate system, the suggestion has been made that a failure of quantal release might actually be determined postsynaptically, i.e. the small number of receptors in a patch might be switched between activatable or inactivatable states quickly. Transmitter released onto a patch with inactivated receptors would be recorded as a transmission failure. We have made additional observations of transmission failures that appear to be more difficult to explain by this hypothesis than the minimal stimulation data.

In five cells, weak stimulation induced IPSCs that were clearly larger than individual quanta and yet transmission still completely failed on occasion and failures of multiquantal release also increased during DSI. In the example shown in Fig. 5*C*, we elicited a single quantal IPSC with a stimulation intensity of 225 μA and observed that failures of transmission occurred during DSI (filled circles). We then increased the stimulation intensity to 275 μA and elicited IPSCs that were approximately three times larger than with the weaker stimulation (open circles). Nevertheless, even with these multiquantal events, complete failures of transmission still increased during DSI. We have observed similar increases in failures with IPSCs having control amplitudes of over −200 pA.

Large evoked IPSCs consist of multiquantal components

More frequently we noted that monosynaptically evoked IPSCs hundreds of picoamps in amplitude had distinguishable components that could appear simply as inflection points on the rising or falling phase of the response, or as entities with readily distinguishable onset latencies and amplitudes. In IPSCs evoked from sixteen cells we identified a total of forty-six components, each IPSC having from two to five components. The component amplitudes ranged from −24 to −1149 pA, with a mean

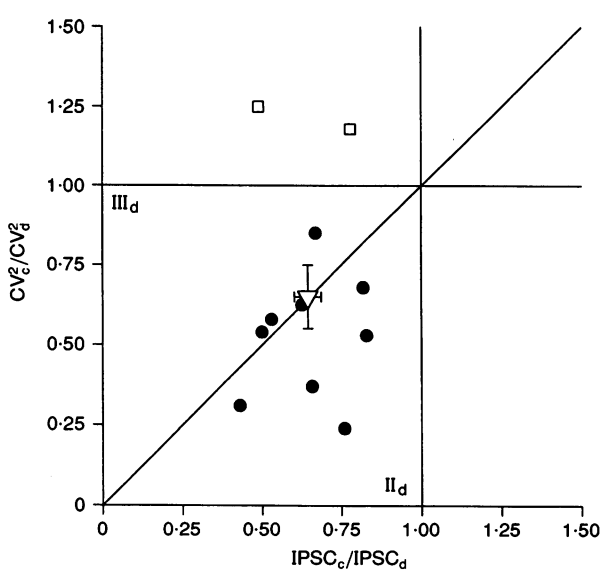

Figure 4. Analysis of coefficient of variation of evoked responses is consistent with a presynaptic mechanism for DSI

The points represent results from cells in which the square of the coefficient of variation (CV^2) of evoked IPSC amplitudes was compared in control conditions and then during DSI (see Methods). The plot shows the ratio of CV^2 before (CV_c^2) and then during DSI (CV_d^2), plotted against the ratio of the mean IPSC amplitudes during DSI compared with control ($IPSC_d/IPSC_c$, i.e. essentially a measure of the magnitude of DSI). Results are from 9 cells in which the coefficient of variation increased during DSI (●); and from those cells in which CV actually decreased during DSI (□, see text for discussion). The mean (with S.E.M.) of all points is shown by ▽. The diagonal line and region II_d represent location of points if the change is purely presynaptic (points in III_d could be either presynaptic or postsynaptic) according to a simple theoretical model; a purely postsynaptic effect would be indicated by points falling on the horizontal line.

and S.E.M. of −294 ± 38·0 pA. In contrast, in six cells the amplitude distributions of TTX-resistant, presumed quantal mIPSCs had means of −18 ± 13·5 pA. Of the evoked IPSC components, only nine were within 3 standard deviations of the mean quantal amplitude (i.e. < −60 pA); the remaining thirty-seven had a mean of −354 ± 41·6 pA and were, accordingly, considered multiquantal. A conservative estimate would be that the average multiquantal component consisted of 15–20 quantal units (e.g. Mody, De Koninck, Otis & Soltesz, 1994). This number roughly agrees with numbers of histologically identified synapses made by a single interneuron onto a pyramidal cell (Buhl, Halasy & Somogyi, 1994). It is also consistent with the numbers of synapses made by a single interneuron based on conductance measurements of either 'unitary' IPSCs obtained by paired, interneuron–pyramidal cell recordings (Miles & Wong, 1984) or from measurements of 'minimal' IPSCs (Lambert & Wilson, 1993). These experiments gave mean single-cell IPSC conductances of 6·5 and 7 nS, respectively, in reasonable agreement with our mean multiquantal IPSC component conductance of ~6 nS. If the probability of quantal release from a single GABA-releasing bouton is approximately 0·5 (Miles & Wong, 1984) then the probability of, e.g., ten independent boutons releasing simultaneously by chance is very low ($P < 0{\cdot}001$). It is much more likely that in this case the boutons are not independent. A multiquantal component would represent the synchronous activation of many synapses made by a single interneuron, or a large branch of an interneuron, onto a given pyramidal cell.

In eleven cells we examined evoked monosynaptic IPSCs having multiquantal components during the DSI period. In nine cells DSI was associated with an apparent all-or-none drop-out of individual components during the DSI period. In two cells the responses became smaller, although there was no obvious drop-out of the individual components. The components were moderate-to-large in amplitude, and their onsets were well separated in time. The clearest example from this group is shown in Fig. 6*A*. In the control period both major components of the IPSC occurred with every stimulus. After a DSI-inducing pulse, the second large component failed nearly 80% of the time, while the first component never did. Following the DSI period the second component recovered fully.

In other cases the IPSC components were not always as well separated from each other temporally (e.g. 6*B*). In this example the components were more numerous and variable than in Fig. 6*A*. In such cases differentiation of the current waveforms (using the Clampfit routine of pCLAMP 6) was used to emphasize the onset time of the various components. Stability in onset of the various components is evident in the overlapping peaks of the differentiated traces. Having identified IPSC components in the differentiated traces, we measured their amplitudes at the appropriate time points on the original individual IPSC current traces. In the example in Fig. 6*B*, the differentiated traces (second row) reveal three major detectable components with distinct onset latencies and maximal rise times (indicated by the arrows). Although not obvious in the traces shown, detailed analysis

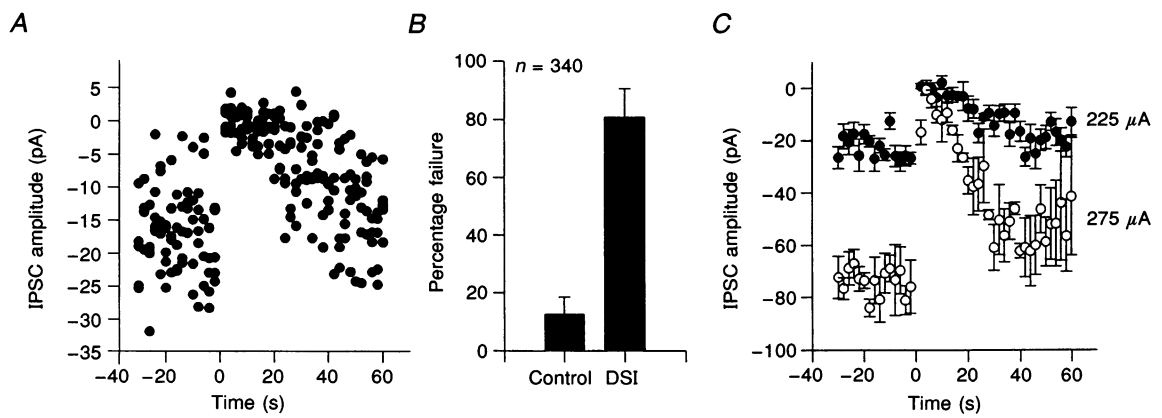

Figure 5. Failures of quantal IPSCs evoked with minimal stimulation to stratum radiatum increase during DSI

A, graph shows IPSC amplitudes of 5 DSI episodes with a 90 mV depolarizing step occurring at time 0 from one cell. Minimal IPSCs, recorded with KCl-filled electrodes, were evoked at 0·5 Hz. Peak amplitude measurements were made in the window from 0 to 14 ms following the extracellular stimulus. For the 10 sweeps immediately prior to the voltage step, the stimulus was ineffective in eliciting an IPSC in only 6 of 50 trials, but failed to elicit a response in 50 of 60 trials during the DSI period. *B*, histogram illustrates percentage failure of transmission during the control and DSI period for 3 cells as in *A*, comparing the 10 traces immediately prior to and following the depolarizing voltage step, for a total of 340 trials. *C*, failures of transmissions during the DSI period were evident when quantal-sized IPSCs were evoked with a stimulus intensity of 225 μA (●), as in *A* (minimal stimulation data from this cell included in *B*). Failures were still observed when larger, multicomponent IPSCs were evoked with a stimulus intensity of 275 μA (○). Data from multicomponent IPSCs not included in histograms in *B*.

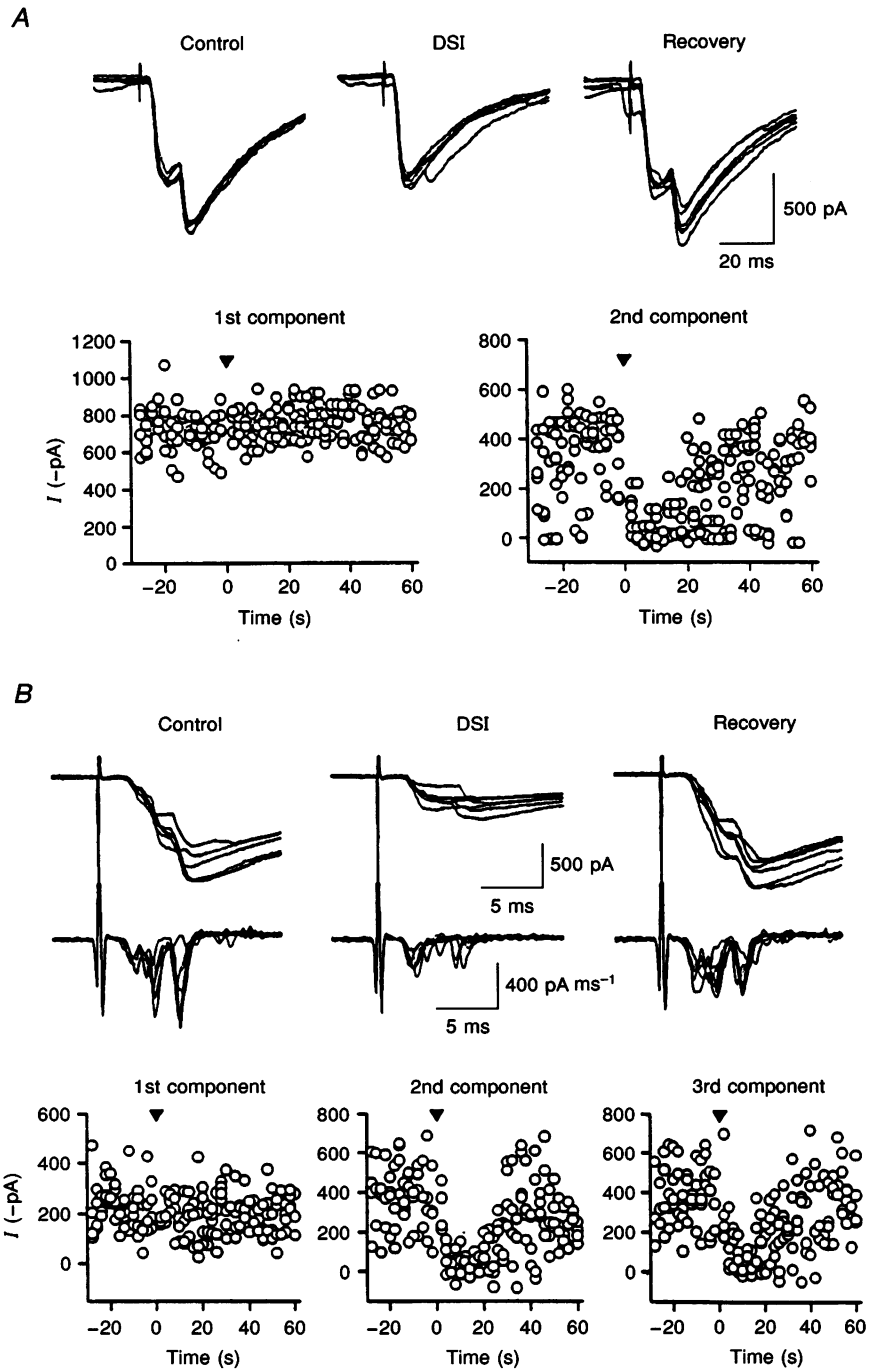

Figure 6. Failures of large, multiquantal evoked IPSC components increase during DSI

A, moderate stimulus intensity evoked an IPSC with two large components. Consecutive individual traces were from control, DSI and recovery periods. Graphs at bottom represent individual response amplitudes for the first and second components throughout the experiment. Depolarizing voltage step delivered at time zero (arrowhead). *B*, in complex responses DSI is also expressed as a dropping out of individual IPSC components. Six consecutive traces evoked at 0·5 Hz in the control period, during DSI and then following recovery from DSI. The middle row illustrates the differentiated waveforms for the traces above. Notice the clustering of IPSC components at a few intervals, as indicated by the superimposition of peaks in the differentiated traces. The graphs below illustrate amplitudes of the individual components, identified by latencies as shown in the middle row. Numerous failures of the second and third components were evident during the DSI period.

revealed additional small units occurring at a stable latency in this cell (see Fig. 7). During the DSI period there was no obvious change in the first component (or second component, not shown), whereas the other major components often failed. Component amplitudes, from many consecutive DSI trials on this cell, are shown in the scatter plots. Notice the relative consistency of component 1 in contrast to the numerous failures (deflections < -10 pA) of components 2 and 3 occurring during the DSI period. Reversible increases in failures were seen during DSI in other cells.

Multiquantal IPSC components tend to occur at stable latencies

If the interpretation is correct that these multiquantal IPSCs represent the synchronized activation of a number of synapses on one cell, then a latency analysis of these components should show fixed peaks. That is, if the components truly represent the simultaneous, non-independent activation of many synapses, then they should occur at stable latencies determined by action potential propagation in the presynaptic cells. If the large components instead represent random co-occurrence of release from many synapses, then stable latency peaks would not be evident. In seven cells we measured latency and amplitude of each discernible component individually from four to eight complete DSI trials per cell. Between 55 and 366 components were identified during the control period in the various cells. In all cells the IPSC components, even as they fluctuated in amplitude, occurred at fixed latencies. In the example shown in Fig. 7, four peaks in the latency distribution were clearly apparent. From the histograms of all seven cells a total of twenty-five distinct latency peaks (2–5 per cell) were identified during the control period for the cells in this group. The mean interval between peaks was $2{\cdot}3 \pm 0{\cdot}38$ ms ($n = 18$). It is clear that the IPSC components occur at fixed latencies. As expected on the hypothesis that DSI involves the selective dropping out of multiquantal IPSC components, there was no change in the latency distribution of the IPSC components during the DSI period. The peaks of the distribution were constant, but there were fewer events in most latency classes. Similar results have been obtained from each of the other six cells analysed.

Distinct peaks in the amplitude histograms of individual components were evident in four of seven cells. In view of the large numbers of synapses involved in multiquantal responses, it is not surprising that distinct peaks are not always obvious since variability in release among individual terminals will tend to obscure sharp peaks. Figure 6*A* shows a cell in which all events between 250 and 500 pA dropped out, whereas events above 600 pA were unchanged. Figure 8 illustrates a more typical instance in

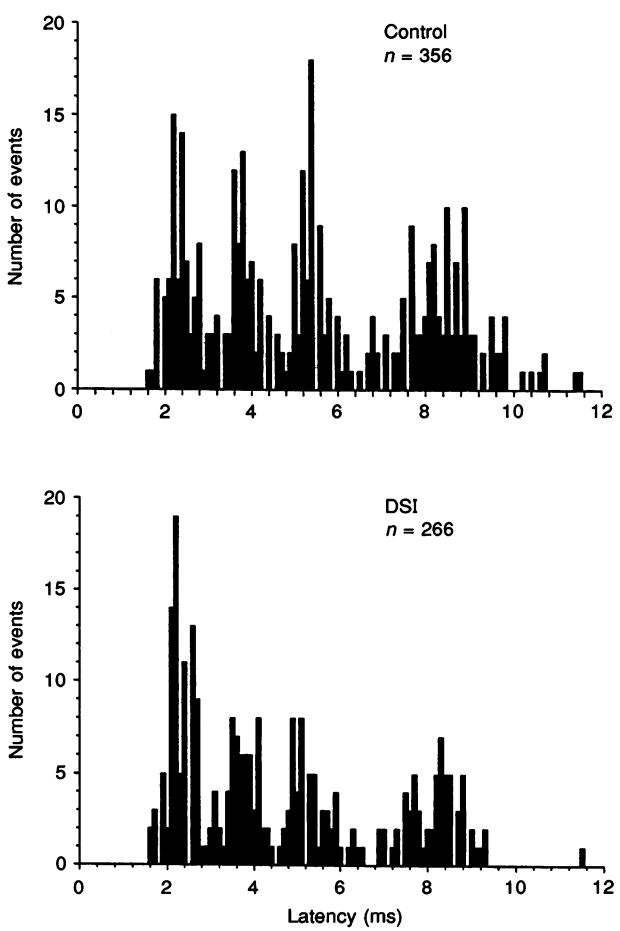

Figure 7. Distribution of onset latencies for individual IPSC components shows stable peaks before and during DSI

Data from 622 distinguishable components from one cell (same cell as in Fig. 6*B*; note the histograms reveal 4 stable peaks, whereas data for only the most prominent were illustrated in the graphs of Fig. 6*B*). DSI of the mean response was 37%. There was a 25% decrease in the total number of discernible components, but no apparent change in the latency distribution.

which there appear to be three peaks, roughly between (absolute values) 100 and 249, 250 and 519, and 520 and 800 pA, in the IPSC component amplitude distribution in the control period. The means of the IPSC components in these ranges were: 178 ± 5·3 pA ($n = 40$), 351 ± 10·4 pA ($n = 45$), and 578 ± 17·7 pA ($n = 14$), respectively, in control and 193 ± 7·1 pA ($n = 32$), 355 ± 9·7 pA ($n = 44$), and 739 ± 34·0 pA ($n = 2$), respectively, during DSI. The mean IPSC suppression in this cell was 33%, and in total there were 20% fewer identifiable IPSC components in the DSI period than in control. During DSI, virtually all components in the range of 520–800 pA were gone, but the number of components between 100 and 250–500 were nearly unchanged. In general, there was no consistent shift in the amplitude distributions of the IPSC component; of the seven cells, the mean of the IPSC component amplitude distributions decreased in three and increased in four. Interestingly, there was a modest positive correlation between the percentage DSI and decrease in number of components ($r = 0·50$). The correlation between percentage DSI and the change in the means of the distributions of IPSC component amplitudes was negligible ($r = 0·12$). The increase in failures of multiquantal IPSCs strongly supports the hypothesis of a presynaptic locus of DSI expression (see below).

Paired-pulse depression of monosynaptic IPSCs does not change during DSI

The data from these various experiments are consistent in pointing to a presynaptic site of expression of DSI. In principle our results would be compatible with either of two DSI mechanisms: reduction of the probability of GABA release determined by factors at the nerve terminal or block of action potential conduction in presynaptic axons. To begin to distinguish between these two possibilities, we examined paired-pulse depression (PPD) of IPSCs during DSI. PPD is the phenomenon whereby the second of a pair of stimuli delivered to GABA-releasing axons elicits a response that is smaller than that elicited by the first stimulus. PPD is measured as the ratio of the second response amplitude to the first and is mediated by a decrease in the probability of release from presynaptic terminals (Davies *et al.* 1990; Nathan & Lambert, 1991; Pitler & Alger, 1994*a*; Wilcox & Dichter, 1994; Lambert & Wilson, 1994). If DSI decreases the probability of transmitter release by affecting factors intrinsic to individual boutons, PPD should decrease during DSI (the less release induced by the first pulse, the more will be induced by the second, hence *less* PPD). However, if DSI reflects axonal conduction block, then, in the simplest model, PPD should be unaffected; although fewer terminals would release

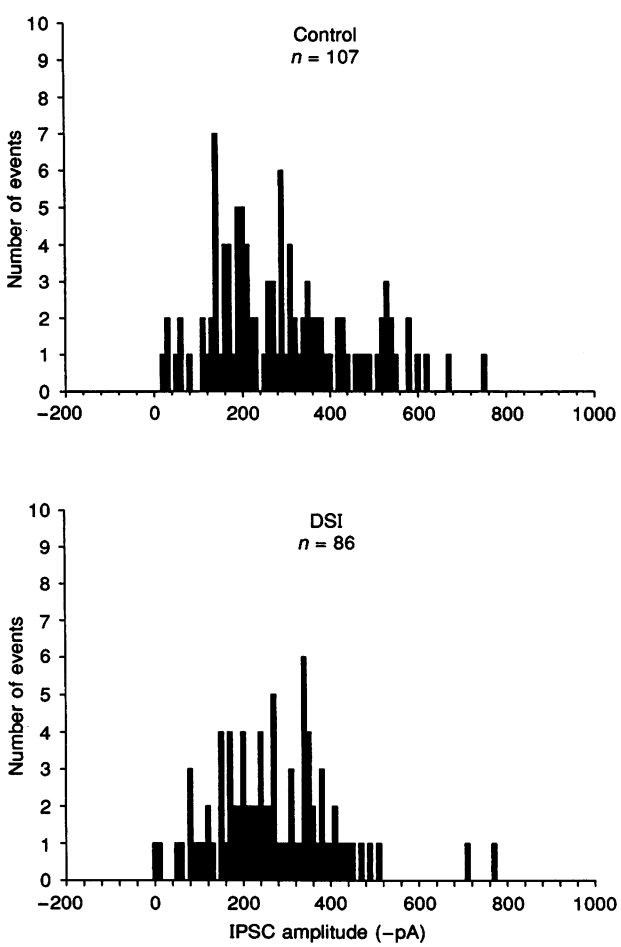

Figure 8. Amplitude distribution of IPSC components during control and DSI periods

Data obtained from one cell during control (top) and DSI periods (bottom). Four complete DSI trials were run and 26 traces collected (13 in control and 13 during DSI) for each. Amplitudes of all distinguishable IPSC components were measured and plotted. There was a 33% decrease in the mean IPSC during DSI in this cell. Note decrease in events > 500 pA. See text for details.

transmitter, the probability of release from any single terminal should not change. We found that PPD does not change during DSI. In five cells, PPD was 0·77 ± 0·03 in control and 0·74 ± 0·02 during DSI ($n = 5$, data not shown). For comparison, we found that 1 μM baclofen, which suppressed IPSCs by an average of 52%, reduced PPD significantly (Davies *et al.* 1990). PPD was 0·61 ± 0·01 in control and 0·83 ± 0·02 in baclofen ($n = 3$). The degree of IPSC suppression by DSI and baclofen was comparable; hence the difference in their effects on PPD strongly suggests a different locus of action. Baclofen acts at interneuron terminals to affect release; thus these results support the hypothesis that the reduction in GABA release during DSI occurs because some interneuron terminals are not invaded by action potentials

DISCUSSION

We previously showed that DSI is induced by postsynaptic factors, such as increased intracellular [Ca^{2+}] (Pitler & Alger, 1992*a*, 1994*b*). The present experiments greatly strengthen the hypothesis that DSI is expressed as a reduction in GABA release and therefore imply that a retrograde signal is required to explain DSI. A lingering concern from previous work was that a postsynaptic decrease in $GABA_A$ receptor responsiveness had been missed. Iontophoretic GABA application had failed to reveal such a decrease (Pitler & Alger, 1992*a*); however, this technique is coarse and might well not have picked up subtle changes restricted to synaptic receptors. While spontaneous, TTX-insensitive mIPSCs undoubtedly provide a sensitive assay of synaptic $GABA_A$ receptors, we could not be certain that the mIPSCs we recorded were actually from synapses at which DSI was expressed. Although there are many $GABA_A$ synapses on a pyramidal cell, the recorded mIPSC frequency is sometimes low (~1 Hz), and it may be that many synapses either release quanta infrequently or not at all (Soltesz *et al.* 1995). In the present work we performed three different types of tests designed to remove these concerns. (1) We massively increased the TTX-resistant mIPSC frequency to try to activate synapses that may have been 'silent' and hence unobservable, but mIPSCs remained unaffected by DSI. (2) We used pharmacological tests and found that 4-AP and veratridine, which could only work on presynaptic elements under our experimental conditions and would in any case have no effect on $GABA_A$ receptors, significantly reduced DSI. Finally, (3) we studied monosynaptically evoked IPSCs to activate synaptic receptors and yet avoid reliance on spontaneous occurrence of IPSCs. Evoked IPSCs were depressed during DSI, and changes in the coefficient of variation were consistent with a presynaptic mechanism. Moreover, failures of synaptic transmission increased during DSI. While occurrence of failures of quantal events has traditionally been accepted as indicative of a presynaptic control mechanism, recent work has led to speculation that the small receptor clusters that mediate quantal synaptic events might be activated or inactivated *en bloc*. Under this scheme, failures of quantal events could conceivably reflect postsynaptic receptor cluster inactivation. As discussed below, a postsynaptic hypothesis is much less plausible in the case of the large multiquantal IPSCs that often occur. Hence, we ascribed particular significance to our observations of multiquantal response failure. Thus, the three types of test pointed to a presynaptic site of DSI expression. Coupled with previous evidence for a postsynaptic induction step, the data continue to support the hypothesis of retrograde signalling.

Study of multiquantal IPSC components during DSI supported several conclusions. (1) DSI involves a decrease in reliability of transmission. (2) Decreased reliability can occur at an anatomical level of complexity greater than a single synapse. (3) Hypothetical regulation of GABA responses at the level of postsynaptic receptor clusters is very unlikely to account for hippocampal DSI. Regulation at the receptor cluster level is nevertheless difficult to rule out entirely (especially if mIPSCs were not from synapses susceptible to DSI). Point (3) now follows from consideration of our findings in light of the morphology of identified interneurons (Gulyas, Miles, Sik, Toth, Tamamaki & Freund, 1993; Buhl *et al.* 1994; Sik, Ylinen, Penttonen & Buzsaki, 1994). If DSI were the result of postsynaptic changes in receptor clusters, the block of multiquantal units would mean that many clusters would have to switch off at the same time. However, it is clear that DSI does not involve a process whereby all postsynaptic $GABA_A$ receptors on a given cell are switched off. The observation that one IPSC component could be blocked while others were not (cf. Figs 6 and 7) would imply a high degree of selectivity on the part of the pyramidal cell, which would have to distinguish and regulate, the synapses made by one interneuron (or branch) while leaving unaltered numerous nearby synapses. With the exception of occasional double release sites, synapses made by a given interneuron onto a pyramidal cell do not occur together in close proximity, but rather spread out over considerable distances (Buhl, Halasy & Somogyi, 1994), intermingled with many synapses from other cells. It is hard to imagine how a hypothetical postsynaptic mechanism could operate given this arrangement. On the other hand, if DSI is caused by a presynaptic reduction in GABA release then the data can easily be explained. Selective blockade of synapses made by only one or two cells or interneuronal branches would occur if the retrograde signal affected only those elements. Geometrical factors such as the varying branching patterns of different interneuronal axons may account for the varying susceptibility of different IPSCs to DSI. Taken together, all our data support the hypothesis that a retrograde signal induced in the postsynaptic cell prevents GABA release from presynaptic boutons.

In hippocampus, DSI may represent a decoupling of presynaptic action potential firing in the interneuron from the process of vesicle release (Pitler & Alger, 1994*b*). However, the hypothesis that the DSI process involves inhibition of presynaptic voltage-dependent Ca^{2+} channels

now seems unlikely because Ca^{2+}-dependent mIPSCs are not reduced during DSI (Fig. 1). Indeed the experiment in Fig. 1 seems to indicate that DSI does not interfere with the asynchronous Ca^{2+}-dependent release process but rather must inhibit synchronous release.

Synchronous release can be regulated by various mechanisms. Synaptotagmin I, a presynaptic protein, is an example of a factor selectively involved in regulation of synchronous Ca^{2+}-dependent release (Geppert *et al.* 1994). Hence, disruption of the synaptotagmin-I-dependent step(s) could theoretically be responsible for DSI. However, it will be a challenge to understand how 4-AP and veratridine could overcome the disruption. On the other hand, synchronous release is also governed by processes that control action potential invasion of the nerve terminal region. Thus DSI could represent action potential conduction block in the complex interneuronal axon plexus (Buhl *et al.* 1994; Sik *et al.* 1994). Both 4-AP and veratridine could restore conduction through a DSI-induced region of low safety factor by prolonging the presynaptic action potential. Axonal conduction block can decrease transmission simultaneously at multiple synapses because all synapses distal to the point of blockade will be prevented from releasing transmitter. If a subset of synapses did not release transmitter because of axonal conduction block, PPD at the remaining, active synapses would be unaltered. Interneuronal axons often run along the pyramidal cell processes and somata in close apposition to them (Buhl *et al.* 1994). A retrograde signal from the pyramidal cell would not have to diffuse far to influence axonal conduction. Variability in susceptibility to DSI would be related to variability in the details of the morphological arrangements between a given interneuron–pyramidal cell pair. It will be interesting to test these hypotheses in future experiments.

We have recently reviewed the evidence for retrograde signalling in DSI in hippocampus and cerebellum (Alger & Pitler, 1995). Despite many similarities there were some different features. In the cerebellum there are both TTX-sensitive and TTX-insensitive DSI processes (Vincent & Marty, 1993), whereas in the hippocampus only the TTX-sensitive form appears to play a significant role (Pitler & Alger, 1994*b*). Our data suggest that axonal conduction failure may represent the TTX-sensitive DSI mechanism in both structures. Recently Vincent & Marty (1996) have obtained additional evidence for axonal branch point conduction failure in simultaneous paired recordings from interneurons and Purkinje cells (A. Marty, personal communication). Their work strongly suggests that action potentials do not consistently invade all synaptic nerve terminals of complex interneuronal arbors and that propagation failures can explain the great variability in monosynaptically evoked IPSCs of cerebellar basket cells. Propagation failure could also explain the similar IPSC variability in hippocampus (e.g. Fig. 5).

While the phenomenon of retrograde transmission at peripheral synapses of vertebrates and invertebrates is widely acknowledged (Jessell & Kandel, 1993; Davis & Murphey, 1994), it is still a controversial topic in the mammalian CNS. In the most prominent example, the evidence for retrograde transmission in long-term potentiation (Bliss & Collingridge, 1993), although suggestive, is not universally accepted (e.g. Manabe & Nicoll, 1994). The work on DSI in hippocampus and cerebellum clearly establishes that retrograde signalling must be considered a genuine neurophysiological mechanism in the mammalian brain.

Alger, B. E. & Pitler, T. A. (1995). Retrograde signaling at $GABA_A$-receptor synapses in the mammalian CNS. *Trends in Neurosciences* **18**, 333–340.

Blanton, M. G., Lo Turco, J. J. & Kriegstein, A. R. (1989). Whole cell recording from neurons in slices of reptilian and mammalian cerebral cortex. *Journal of Neuroscience Methods* **30**, 203–210.

Bliss, T. V. P. & Collingridge, G. L. (1993). A synaptic model of memory: long-term potentiation in the hippocampus. *Nature* **361**, 31–39.

Buhl, E. H., Halasy, K. & Somogyi, P. (1994). Diverse sources of hippocampal unitary inhibitory postsynaptic potentials and the number of synaptic release sites. *Nature* **368**, 823–828.

Chen, Q. X., Stelzer, A., Kay, A. R. & Wong, R. K. S. (1990). $GABA_A$ receptor function is regulated by phosphorylation in acutely dissociated guinea-pig hippocampal neurones. *Journal of Physiology* **420**, 207–221.

Cutler, R. W. P. & Young, J. (1979). The effect of penicillin on the release of gamma-aminobutyric acid from cerebral cortex slices. *Brain Research* **170**, 157–163.

Davies, C. H., Davies, S. N. & Collingridge, G. L. (1990). Paired-pulse depression of monosynaptic GABA-mediated inhibitory postsynaptic responses in rat hippocampus. *Journal of Physiology* **424**, 513–531.

Davis, G. W. & Murphey, R. K. (1994). Long-term regulation of short-term transmitter release properties: retrograde signaling and synaptic development. *Trends in Neurosciences* **17**, 9–13.

Doze, V. A., Cohen, G. A. & Madison, D. V. (1995). Calcium channel involvement in $GABA_B$ receptor-mediated inhibition of GABA release in area CA1 of the rat hippocampus. *Journal of Neurophysiology* **74**, 43–53.

Edwards, F. (1991). LTP is a long term problem. *Nature* **350**, 271–272.

Edwards, F. A., Konnerth, A. & Sakmann, B. (1990). Quantal analysis of inhibitory synaptic transmission in the dentate gyrus of rat hippocampal slices: a patch-clamp study. *Journal of Physiology* **430**, 213–249.

Faber, D. S. & Korn, H. (1991). Applicability of the coefficient of variation method for analyzing synaptic plasticity. *Biophysical Journal* **60**, 1288–1294.

Geppert, M., Goda, Y., Hammer, R. E., Li, C., Rosahl, T. W., Stevens, C. F. & Sudhof, T. C. (1994). Synaptotagmin I: a major Ca^{2+} sensor for transmitter release at a central synapse. *Cell* **79**, 717–727.

GULYAS, A. I., MILES, R., SIK, A., TOTH, K., TAMAMAKI, N. & FREUND, T. F. (1993). Hippocampal pyramidal cells excite inhibitory neurons through a single release site. *Nature* **366**, 683–687.

JESSELL, T. M. & KANDEL, E. R. (1993). Synaptic transmission: a bidirectional and self-modifiable form of cell-cell communication. *Neuron* **10** (suppl.), 1–30.

LAMBERT, N. A. & WILSON, W. A. (1993). Heterogeneity in presynaptic regulation of GABA release from hippocampal inhibitory neurons. *Neuron* **11**, 1057–1067.

LAMBERT, N. A. & WILSON, W. A. (1994). Temporally distinct mechanisms of use-dependent depression at inhibitory synapses in the rat hippocampus in vitro. *Journal of Neurophysiology* **72**, 121–130.

LLANO, I., LERESCHE, N. & MARTY, A. (1991). Calcium entry increases the sensitivity of cerebellar Purkinje cells to applied GABA and decreases inhibitory synaptic currents. *Neuron* **6**, 565–574.

MCNAMARA, J. O. (1994). Cellular and molecular basis of epilepsy. *Journal of Neuroscience* **14**, 3413–3425.

MANABE, T. & NICOLL, R. A. (1994). Long-term potentiation: evidence against an increase in transmitter release probability in the CA1 region of the hippocampus. *Science* **265**, 1888–1892.

MILES, R. & WONG, R. K. S. (1984). Unitary inhibitory synaptic potentials in the guinea-pig hippocampus *in vitro*. *Journal of Physiology* **356**, 97–113.

MODY, I., DE KONINCK, Y., OTIS, T. S. & SOLTESZ, I. (1994). Bridging the cleft at GABA synapses in the brain. *Trends in Neurosciences* **17**, 517–525.

NATHAN, T. & LAMBERT, J. D. C. (1991). Depression of the fast IPSP underlies paired-pulse facilitation in area CA1 of the rat hippocampus. *Journal of Neurophysiology* **66**, 1704–1715.

NICOLL, R. A. & ALGER, B. E. (1981). A simple chamber for recording from submerged brain slices. *Journal of Neuroscience Methods* **4**, 153–156.

PITLER, T. A. & ALGER, B. E. (1992*a*). Postsynaptic spike firing reduces synaptic $GABA_A$ responses in hippocampal pyramidal cells. *Journal of Neuroscience* **12**, 4122–4132.

PITLER, T. A. & ALGER, B. E. (1992*b*). Cholinergic excitation of GABAergic interneurons in the rat hippocampal slice. *Journal of Physiology* **450**, 127–142.

PITLER, T. A. & ALGER, B. E. (1994*a*). Differences between presynaptic and postsynaptic $GABA_B$ mechanisms in rat hippocampal pyramidal cells. *Journal of Neurophysiology* **72**, 2317–2327.

PITLER, T. A. & ALGER, B. E. (1994*b*). Depolarization-induced suppression of GABAergic inhibition in rat hippocampal pyramidal cells: G protein involvement in a presynaptic mechanism. *Neuron* **13**, 1447–1455.

PITLER, T. A., ALGER, B. E., WAGNER, J. J. & LENZ, R. A. (1995). Retrograde signalling and possible axonal conduction block in depolarization-induced suppression of inhibition in rat hippocampal cells. *Society for Neuroscience Abstracts* **21**, 1521.

SIK, A., YLINEN, A., PENTTONEN, M. & BUZSAKI, G. (1994). Inhibitory CA1-CA3-hilar region feedback in the hippocampus. *Science* **265**, 1722–1724.

SOLTESZ, I., SMETTERS, D. K. & MODY, I. (1995). Tonic inhibition originates from synapses close to the soma. *Neuron* **14**, 1273–1283.

STELZER, A. (1992). $GABA_A$ receptors control the excitability of neuronal populations. *International Review of Neurobiology* **33**, 195–287.

STELZER, A., SIMON, G., KOVACS, G. & RAI, R. (1994). Synaptic disinhibition during maintenance of long-term potentiation in the CA1 hippocampal subfield. *Proceedings of the National Academy of Sciences of the USA* **91**, 3058–3062.

STORM, J. F. (1988). Temporal integration by a slowly inactivating K^+ current in hippocampal neurons. *Nature* **336**, 379–381.

THOMPSON, S. M. (1994). Modulation of inhibitory synaptic transmission in the hippocampus. *Progress in Neurobiology* **42**, 575–609.

VINCENT, P., ARMSTRONG, C. M. & MARTY, A. (1992). Inhibitory synaptic currents in rat cerebellar Purkinje cells: modulation by postsynaptic depolarization. *Journal of Physiology* **456**, 453–471.

VINCENT, P. & MARTY, A. (1993). Neighboring cerebellar Purkinje cells communicate via retrograde inhibition of common presynaptic interneurons. *Neuron* **11**, 885–893.

VINCENT, P. & MARTY, A. (1996). Fluctuations of inhibitory postsynaptic currents in Purkinje cells from rat cerebellar slices. *Journal of Physiology* **494**, 183–199.

WIGSTROM, H. & GUSTAFSSON, B. (1983). Facilitated induction of hippocampal long-lasting potentiation during blockade of inhibition. *Nature* **301**, 603–604.

WILCOX, K. S. & DICHTER, M. A. (1994). Paired pulse depression in cultured hippocampal neurons is due to a presynaptic mechanism independent of $GABA_B$ autoreceptor activation. *Journal of Neuroscience* **14**, 1775–1788.

Acknowledgements

This work was supported by NIH grants NS30219 and NS22010 to B.E.A.; L.M. was supported by NIH Neurosciences Training Grant NS07375; and R.L. was supported by the Membrane Training Program T32-GM08181 at the University of Maryland School of Medicine. We thank Evelyn Elizabeth for typing the manuscript and for editorial assistance.

Received 1 September 1995; accepted 13 June 1996.